

# NAVAL POSTGRADUATE SCHOOL

## Monterey, California



## THESIS

### DIGITAL DATA ACQUISITION FOR LASER RADAR FOR VIBRATION ANALYSIS

by

Felix G. Montes

June 1998

Thesis Advisor:

Co-Advisor:

Robert C. Harney

D. Scott Davis

Approved for public release; distribution is unlimited.

19980803 053

# REPORT DOCUMENTATION PAGE

Form Approved  
OMB No. 0704-0188

Public reporting burden for this collection of information is estimated to average 1 hour per response, including the time for reviewing instruction, searching existing data sources, gathering and maintaining the data needed, and completing and reviewing the collection of information. Send comments regarding this burden estimate or any other aspect of this collection of information, including suggestions for reducing this burden, to Washington headquarters Services, Directorate for Information Operations and Reports, 1215 Jefferson Davis Highway, Suite 1204, Arlington, VA 22202-4302, and to the Office of Management and Budget, Paperwork Reduction Project (0704-0188) Washington DC 20503.

1. AGENCY USE ONLY (Leave blank)

2. REPORT DATE  
June 1998

3. REPORT TYPE AND DATES COVERED  
Master's Thesis

4. TITLE AND SUBTITLE  
DIGITAL DATA ACQUISITION FOR LASER RADAR FOR VIBRATION ANALYSIS

5. FUNDING NUMBERS

6. AUTHOR(S)  
Montes, Felix G.

7. PERFORMING ORGANIZATION NAME(S) AND ADDRESS(ES)  
Naval Postgraduate School  
Monterey, CA 93943-5000

8. PERFORMING  
ORGANIZATION REPORT  
NUMBER

9. SPONSORING / MONITORING AGENCY NAME(S) AND ADDRESS(ES)

10. SPONSORING /  
MONITORING  
AGENCY REPORT NUMBER

## 11. SUPPLEMENTARY NOTES

The views expressed in this thesis are those of the author and do not reflect the official policy or position of the Department of Defense or the U.S. Government.

12a. DISTRIBUTION / AVAILABILITY STATEMENT  
Approved for public release; distribution unlimited.

12b. DISTRIBUTION CODE

## 13. ABSTRACT:

Laser radar for vibration analysis represents a military application to develop a target identification system in the future. The problem addressed is how to analyze the vibrations of a target illuminated by the laser radar to achieve a positive identification. This thesis develops a computer-based data acquisition and analysis system for improving the laser radar capability. Specifically, a review is made of the CO<sub>2</sub> laser radar, coherent detection, and data acquisition software and signal processing. These aspects form the basis for a laser radar system, using LabView software for data acquisition and signal analysis, which is capable of detecting vibrations from a stationary target. The laser radar was able to detect the frequencies of vibration of a test target. All the data can be recorded by the system. The laser radar presented could be used for further development and production of a target identification system.

14. SUBJECT TERMS  
CO<sub>2</sub> laser radar, laser radar equations, vibration detection, optics, acousto-optic shift, target identification, detectors, data acquisition

15. NUMBER OF  
PAGES  
56

16. PRICE CODE

17. SECURITY CLASSIFICATION  
OF REPORT  
Unclassified

18. SECURITY CLASSIFICATION OF  
THIS PAGE  
Unclassified

19. SECURITY CLASSIFI- CATION  
OF ABSTRACT  
Unclassified

20. LIMITATION  
OF ABSTRACT  
UL

NSN 7540-01-280-5500

Standard Form 298 (Rev. 2-89)  
Prescribed by ANSI Std. Z39-18  
298-102



Approved for public release; distribution is unlimited

**DIGITAL DATA ACQUISITION FOR  
LASER RADAR FOR VIBRATION ANALYSIS**

Felix G. Montes  
Lieutenant Commander, Venezuelan Navy  
B.S., Venezuelan Naval Academy, 1983

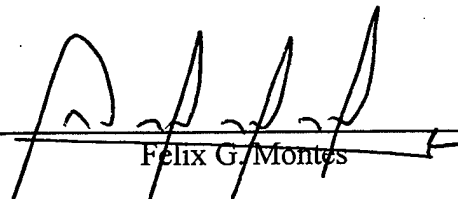
Submitted in partial fulfillment of the  
requirements for the degree of

**MASTER OF SCIENCE IN APPLIED PHYSICS**

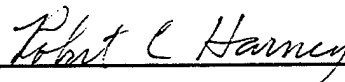
from the

**NAVAL POSTGRADUATE SCHOOL  
June 1998**

Author:

  
Felix G. Montes

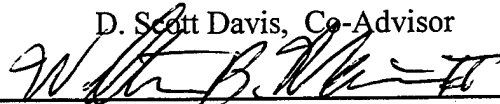
Approved by:



Robert C. Harney, Thesis Advisor



D. Scott Davis, Co-Advisor



William Maier II, Chairman  
Department of Physics



## ABSTRACT

Laser radar for vibration analysis represents a military application to develop a target identification system in the future. The problem addressed is how to analyze the vibrations of a target illuminated by the laser radar to achieve a positive identification.

This thesis develops a computer-based data acquisition and analysis system for improving the laser radar capability. Specifically, a review is made of the CO<sub>2</sub> laser radar, coherent detection, and data acquisition software and signal processing.

These aspects form the basis for a laser radar system, using LabView software for data acquisition and signal analysis, which is capable of detecting vibrations from a stationary target. The laser radar was able to detect the frequencies of vibration of a test target. All the data can be recorded by the system.

The laser radar presented could be used for further development and production of a target identification system.



## TABLE OF CONTENTS

I. INTRODUCTION.....	1
II. LASER RADAR.....	3
A. CONFIGURATION.....	3
B. LASER RADAR EQUATION.....	5
C. VIBRATION DETECTION.....	7
D. CO <sub>2</sub> LASER .....	11
E. OPTICS .....	15
F. ACOUSTO-OPTIC SHIFT .....	17
G. TARGET .....	19
H. DETECTOR .....	20
I. SIGNAL PROCESSING ELECTRONICS.....	21
III. DATA ACQUISITION.....	23
A. VIRTUAL INSTRUMENT .....	23
B. HARDWARE.....	25
C. SOFTWARE .....	29
IV. EXPERIMENTAL SET UP.....	33
A. LASER RADAR SET UP AND OPERATING PROCEDURES .....	33
V. OBSERVATIONS AND RESULTS .....	35
VI. CONCLUSIONS.....	41
VII. RECOMMENDATIONS.....	43
LIST OF REFERENCES .....	45
INITIAL DISTRIBUTION LIST.....	47



## I. INTRODUCTION

The military application of a laser radar system as a vibration sensor has gained importance recently because its high resolution information can be used in the target identification process.

Vibrational signature identification of both aircraft and ground vehicles has the potential for combat identification. The laser radar is capable of higher accuracy and greater sensitivity to internal vibrations than other systems.

In this project a computer-based instrument is added to an existing laser radar system. Specifically, the project covers the application of a data acquisition (DAQ) system, which processes and analyzes the analog signal coming from a CO<sub>2</sub> laser radar, and displays the results in a virtual instrument panel. LabView is the software chosen for this research, because it combines high-speed operation, power spectrum diagnostics, and collection of data. Using the appropriate interface hardware, users can configure a broad range of programmable instruments, with data acquisition, recording and data analysis capability.

The hardware interface chosen is a National Instruments PC-516 plug-in board, which improved the computer processing capabilities, making the laser radar platform more portable and better for data acquisition applications. The PC-516 was programmed using the data acquisition driver software (NI-DAQ) provided.



## II. LASER RADAR

### A. CONFIGURATION

The laser radar has the capability to measure a laboratory target's vibrations, and it is the signal generator for the DAQ system. This thesis covers the combination of the laser radar and the processing computational unit.

The radar is a 10 W, 10.6  $\mu\text{m}$  wavelength,  $\text{CO}_2$  laser-based system, which detects and measures frequencies and amplitudes of a controlled vibration laboratory target, in the frequency range of 1 Hz - 20 kHz. The nominal frequency for this experiment was 400 Hz.

This device has better angular, range and velocity resolution than the traditional RF radars because of the shorter wavelengths used. The vibration detecting process requires measuring the relative phase between two electromagnetic waves of the same frequency and polarization. In this case, the reference (local oscillator) wave travels a fixed distance, while the other travels to the target. When the latter returns, it is combined with the first, and the resulting signal is a function of the relative phase of the two waves, which changes as the target vibrates.

The relative phase is inversely proportional to the wavelength, and smaller wavelengths are the best for small distance resolution. This process is called "homodyne" coherent detection. Adding a small frequency shift to one of the waves gives to the device the "offset homodyne" configuration that lets it detect small amplitude vibrations of stationary targets.

The signal obtained is sent to a signal-processing unit. In our laser radar the frequency of the target beam is shifted, in addition to the vibration frequency shift, by an acousto-optic modulator at 30 MHz. The radar filters and amplifies the signal from the detector before signal processing.

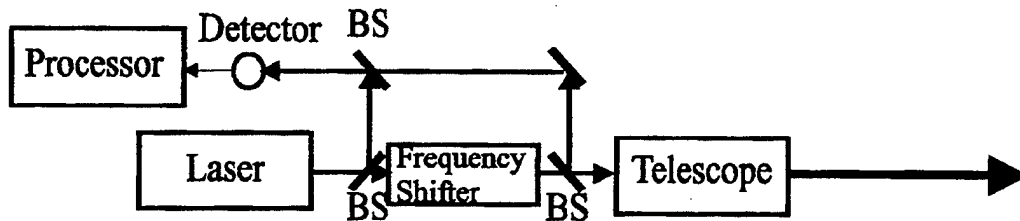


Fig. 1 Offset homodyne configuration of the laser radar (Day, 1997).

The radar is mounted on a TMC optical breadboard to attenuate vibrations and to optimize optical system performance.

The IntraAction acousto-optic modulator (AOM) imposes a 30 MHz frequency shift on the laser beam and is driven by a 30W-30MHz IntraAction modulator driver power supply. The AOM provides an emergency cutoff in case of overheat.

The optical system is made of zinc selenide lenses. The optics transmits as much laser light as possible. The transmitter optical efficiency is 21 %, and the optical receiving efficiency is 52 %.The optical alignment is very critical.

The target is a retroreflector configuration, bonded to a ThorLabs piezoelectric actuator that allows 17.4  $\mu\text{m}$  of displacement when driven by a 150V signal given by a ThorLabs single channel piezoelectric driver.

The detection system consists of a room temperature semiconductor HgCdTe detector, a high frequency amplifier, and electronics circuitry. The detector has an effective photoconductive gain that depends on the bias voltage applied and the detector area. The specific detectivity ( $D^*$ ) of the detector is equal to  $6.7 \times 10^6 \text{ cm}\sqrt{\text{Hz/W}}$  at room temperature.

The responsivity of the detector is 100 mV/W with a +10V bias voltage applied. A Melles Griot high frequency amplifier model 13AMP007 is used to amplify the signal from the detector. The electronics circuitry consists of a series of filters added to limit the frequency response of the radar system. An amplitude limiter and frequency discriminator convert the FM portion of the signal into an AM voltage signal. The target signal is then analyzed in a virtual spectrum analyzer.

## B. LASER RADAR EQUATION

The laser radar equation is based on the physics of the system. This equation expands upon the carrier-to-noise ratio (CNR) of the detector, including the effects of the components of the system. All of these effects can be added to the detector CNR equation to describe a CNR for the system. The CNR is used to determine how much incoming signal is needed to be distinguishable from the noise in the detector. The CNR is the equivalent to the microwave radar definition of signal-to-noise ratio (SNR). The parameters that affect the laser radar performance are: detector parameters, components parameters, light beam fluctuations to the target, reflection off the target, return to the detector, noise, atmospheric turbulence and attenuation.

The CNR laser radar equation depends on the detector quantum efficiency, the transmit and receive path optics transmission efficiencies, the Gaussian spot size at the transmitting aperture of the laser radar, the atmospheric attenuation coefficient, the target reflectivity and radius, light frequency, the range to the target and the electronic bandwidth. For laser radar the CNR is defined as (Harney,1993):

$$\text{CNR} = \frac{\eta_D \epsilon_T \epsilon_R P_T e^{-2\alpha R}}{hfB} \left( \frac{\rho w_o^2}{R^2} \right) \left[ 1 - e^{-\frac{4\pi w_o^2 r_t^2}{\lambda R^2}} \right]$$

CNR = Carrier – to – noise ratio,

$\eta_D$  = Detector quantum efficiency,

$\epsilon_T, \epsilon_R$  = Transmit (receive) paths optics efficiency,

$P_T$  = Incident power on target,

$\alpha$  = Atmospheric attenuation coefficient,

$R$  = Range to the target,

$h$  = Planck's constant,

$f$  = Frequency of light,

$\rho$  = Target reflectivity,

$w_o$  = Gaussian spot size,

$r_t$  = Target radius,

$\lambda$  = Wavelength of light,

$B$  = Electronic bandwidth.

There are two relevant limiting cases of this equation :

**1. Short Range: resolved target (Harney,1993)**

$$CNR = \frac{\eta_d \epsilon_T \epsilon_R P_T e^{-2\alpha R}}{hfB} \left( \frac{\rho w_o^2}{R^2} \right).$$

In this case the target is larger than the laser spot size at the target's range.

**2. Long Range: unresolved target (Harney,1993)**

$$CNR = \frac{\eta_D \epsilon_T \epsilon_R P_T^{-2\alpha R}}{hfB} \left( \frac{4 \pi^2 \rho r_T^2 w_o^4}{\lambda^2 R^4} \right).$$

In this case the target is smaller than the laser spot size at the target's range. The maximum theoretical range applying the resolved target equation is 6.5 km, given the parameters of the current laser radar system. The target reflectivity was assumed to be about 0.1.

## C. VIBRATION DETECTION

### 1. Superposition and Interference

The relative phase difference between two added light beams determines if the interference is constructive or destructive. In this case we are adding two laser beams at the detector, the reference or local oscillator beam and the returned shifted from the target beam.

The two electromagnetic fields with phases  $\phi_1$  and  $\phi_2$  are (Scrubby,1990):

$$E_1 = E_{10} \cos(2\pi\nu t + \phi_1),$$

$$E_2 = E_{20} \cos(2\pi\nu t + \phi_2).$$

The total field is:

$$E_T = E_1 + E_2.$$

The detector responds to the changes in intensity of light  $I$ , which is proportional to the average of the square of the total electrical field (Scrubby,1990):

$$I \propto \sqrt{E_T^2}.$$

The total intensity of light at the detector is (Scrubby,1990):

$$I_T = I_1 + I_2 + 2 (I_1 I_2)^{\frac{1}{2}} \cos(\phi_1 - \phi_2).$$

In our case the phase of the second beam is constant and equal to zero, because the reference beam travels a known fixed distance. The phase of the beam that travels a distance  $d$  to the target is proportional to the number of wavelengths on the total path distance  $D$ :

$$\phi_1 = 2\pi \frac{D}{\lambda} = 4\pi \frac{d}{\lambda},$$

$d = R$  = Distance or range to the target,

$D$  = Total distance the light beam has to travel  
to the target and back.

The target is at normal incidence, and sinusoidally vibrating with amplitude  $a$  and frequency  $f_t$ , then the phase is:

$$\phi_1 = 4\pi \frac{a}{\lambda} \sin(2\pi f_t t).$$

Then we have a relation between the distance, vibration amplitude and frequency of the target and the phase of the target beam. In this case the total intensity is:

$$I_T = I_1 + I_2 + 2(I_1 I_2)^{\frac{1}{2}} \cos\{4\pi \frac{a}{\lambda} \sin(2\pi f_t t)\}.$$

The target vibrations produce variations in the total intensity, that is, the displacement of the target modulates the amplitude of the detected signal at target's vibration frequency. If the frequency of the light beam directed to the target is shifted, using an acousto-optics modulator (AOM) at 30 MHz, the intensity is modulated as function of the amplitude and frequency of the vibration, like a frequency modulated signal. If the amplitude of the target's vibration is small it fits into a narrow band frequency modulation.

The light beams used are coherent, parallel and coincident to let the interference at the detector occur. The coincidence let both light beams reach the same place at the detector, out of parallelism just by no more than a very small angle, creating interference across the whole detector. The optics system and the correct alignment permit this task to be accomplished effectively.

## 2. Frequency Shifting

The frequency of the beam directed to the target is shifted by a convenient frequency. The phase of the beam shifted and reflected from the target is:

$$\phi_1 = 2\pi f_s t + 4\pi \frac{a}{\lambda} \sin(2\pi f_t t),$$

$$f_s = \text{Frequency shift caused by the modulator.}$$

Therefore, the total intensity is:

$$I_T = I_1 + I_2 + 2(I_1 I_2)^{\frac{1}{2}} \cos(2\pi f_s t + 4\pi \frac{a}{\lambda} \sin(2\pi f_t t)).$$

$$\text{The modulation index} = 4\pi \frac{a}{\lambda}.$$

Then the total intensity is going to vary with time, centered at the shift frequency. This is similar to a frequency-modulated signal, when this inequality holds:

$$2\pi f_s t \geq 4\pi \frac{a}{\lambda} \sin(2\pi f_i t).$$

### 3. Intensity Frequency Modulation

The amplitude of the target vibration is small. This means that, to lowest order, the frequency spectrum of the resulting spectrum consists primarily of the target vibration frequency and a single pair of side bands at that frequency plus or minus the shift frequency. This is called narrow band FM (Scrubby, 1990).

### 4. Angular Alignment

To measure the interference of the two beams at the detector, they must be coherent, coincident, and as parallel as possible. To have maximum efficiency, the beam width must be less than half the fringe spacing. Then, the maximum angle is:

$$\beta = \frac{\lambda}{2 D_b},$$

$$D_d = \text{Beam width.}$$

It was found experimentally that the maximum parallel angle is less than 5.3 mrad. The spacing of the fringes over detector is:

$$S = \frac{\lambda}{2 \sin(\frac{1}{2} \beta)} \approx \frac{\lambda}{\beta}.$$

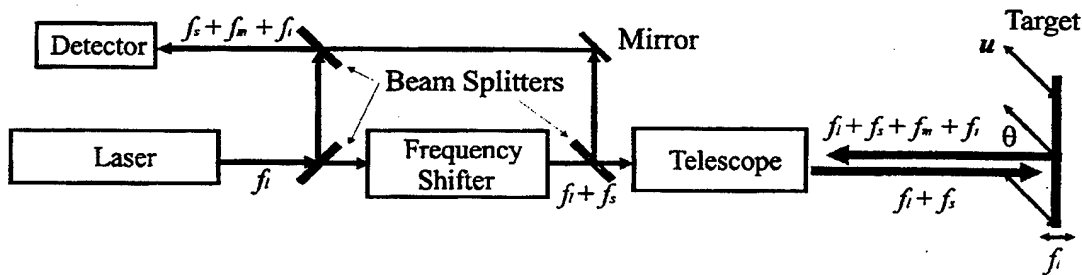


Fig.2 Frequency shifting and vibration detection of the laser radar (Harney, 1993).

In case of target motion  $f_m$  would be the Doppler shift.

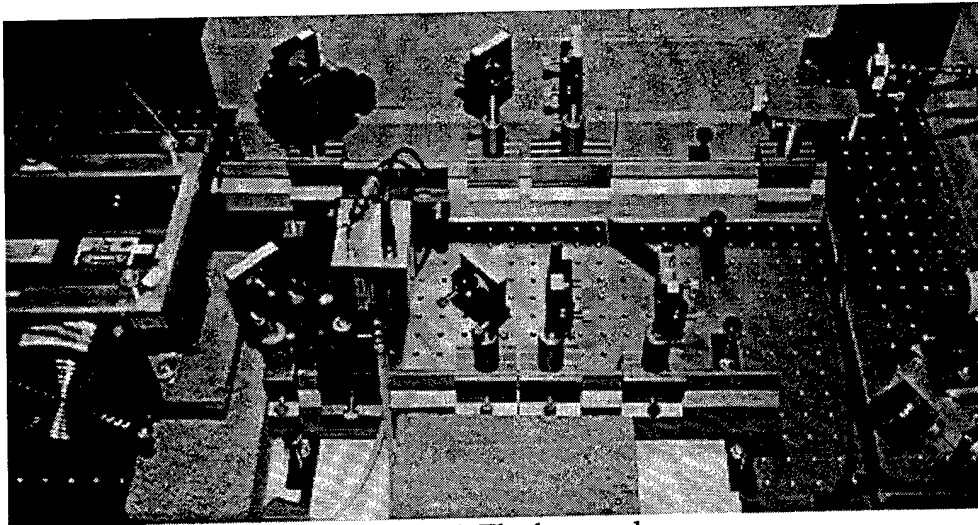


Fig. 3 The laser radar

## D. CO<sub>2</sub> LASER

### 1. Laser Process: Excitation and Emission

The Synrad model G-48-1-28 (W) is a stable oscillator that amplifies coherent light, at 10.6  $\mu\text{m}$  wavelength (frequency  $28.3 \times 10^{12}$  Hz), in continuous wave (CW) mode up to 10 W.

The excitation of the laser begins by the transfer of electrical energy to the N<sub>2</sub> pumping medium. The RF power supply converts the DC power into a 1000 V<sub>pk</sub> RF power, at a frequency of 45 MHz. The oscillating electric field transfers the energy through electronic ionization, gas heating and vibration excitation to the plasma, that contains CO<sub>2</sub>, N<sub>2</sub>, He and others inert gases (Synrad Inc., 1996). The initial gas mixture is typically 67% He, 13% N<sub>2</sub>, 13% CO<sub>2</sub>, and about 7% Xe. The operating gas mixture also contains CO, O, and O<sub>3</sub>, the latter two converting back to O<sub>2</sub> when the plasma shut off.

The first two processes produce free electrons, maintaining the discharge, and accelerate them. These fast electrons collide elastic and inelastically with the neutral molecules of the gas mixture, exciting vibration and rotation states. Vibrational energy is preferentially transferred from N<sub>2</sub> to one specific vibration of CO<sub>2</sub>. CO<sub>2</sub> molecules have three vibrational modes, and changing from one to another, can release energy by spontaneous emission of a photon. The vibrational transition from 001 state to 100 state produces the 10.6  $\mu\text{m}$  lasing wavelength.

During the stimulated emission, an incoming photon stimulates the excited CO<sub>2</sub> molecule to give off a second photon and drop to a lower energy level. The stimulated photon has the same direction, frequency, phase and polarization as the inducing photon, producing coherent light. As the photons travel in the lasing medium they stimulate other CO<sub>2</sub> excited molecules producing photon emission and intensity gain, the amount depending on frequency and distance.

The laser radiation is then amplified using feedback in a gain medium sandwiched between two mirrors. The gain must overcome the losses in the medium, in order to oscillate and amplify. As the amplification increases the CO<sub>2</sub> molecules drop to the lower state. This decreases the number of molecules available for amplification. Eventually gain reaches the saturation point, and the laser is in equilibrium. The frequency width of the Synrad laser due to the line shape effect is 375 MHz (Synrad Inc., 1996). Thermal expansion of the laser resonator can cause a wavelength shift from 10.6  $\mu\text{m}$  to 10.57  $\mu\text{m}$  or 10.63  $\mu\text{m}$ , by forcing a different rotational line to undergo oscillation and amplification.

The Synrad laser has mode purity for the lowest mode TEM<sub>00</sub> of 98 %, and the full angle divergence of the beam at the exit aperture is 4 mrad.

The 10.5 % maximum efficiency power output of the Synrad laser is obtained when the voltage input is between 21 and 24 V, giving the corresponding power output values 10.6 and 12.6 W. However, the maximum power out produced is 14.5 W at 28.4 V input, but the efficiency is only 9.5 %.

As the photons travel across the lasing medium they may find other CO<sub>2</sub> molecules in excited state, which will again produce stimulated emission photons, improving the gain produced over the length of the cavity, as in the following equation (Verdeyen,1995):

$$\frac{dI_v}{dz} = \left[ A_{21} \frac{\lambda^2}{8\pi n^2} g(v) \right] \left[ N_2 - \frac{g_2}{g_1} N_1 \right] I_v = \gamma(v) I_v,$$

$A_{21}$  = Spontaneous emission coefficient,

$\lambda$  = Wavelength of emitted radiation,

$N_1, N_2$  = Number per unit volume of CO<sub>2</sub> molecules in corresponding energy level,

$g(v)$  = Lineshape function,

$\gamma(v)$  = Gain coefficient,

$g_1, g_2$  = Degeneracy factor,

$n$  = Index of refraction,

$I_v$  = Intensity at a frequency  $v$ .

For net gain to occur, both terms in brackets in the latter equation must be positive. Then for laser gain, it follows that there is a population inversion requirement, as in the following equation (Verdeyen,1995):

$$\frac{N_2}{N_1} \geq \frac{g_2}{g_1}.$$

## 2. Feedback, Oscillation and Amplification Process

In order to achieve a large gain, a long column of lasing medium would be required. This requirement can be circumvented by repeatedly feeding the radiation back through the same medium. The CO<sub>2</sub> gain medium is placed between two mirrors, and the gain obtained will depend of the length of the cavity (Verdeyen,1995):

$$G_o = e^{\gamma l},$$

$l$  = Length of the cavity.

The threshold of oscillation depends of the reflectance of the mirrors (Verdeyen,1995):

$$R_1 R_2 e^{2\gamma l} \geq 1,$$

$R_1, R_2$  = Reflectance of mirrors.

When the gain reaches the saturation point, the pumping process is exactly balanced by the emission process, and the laser goes to steady-state.

To achieve usable gain, the mirror cavity must resonant at the laser frequency, with the following conditions (Harney,1996):

$$0 \leq g_1 g_2 \leq 1,$$

$$g_1 = 1 - \frac{1}{r_1},$$

$$g_2 = 1 - \frac{1}{r_2},$$

$r_1, r_2$  mirrors' radii of curvature.

This Synrad laser has a stable configuration with  $g_1 g_2 = 0.886$ .

The distance between mirrors to let the oscillation occur must be (Wilson,1989):

$$L = p \frac{\lambda}{2},$$

$L$  = optical pathlength,

$\lambda$  = wavelength,

$p$  = axial mode of the cavity.

And the cavity mode frequency separation must be (Wilson,1989):

$$\Delta\nu = \frac{c}{2L},$$

$c$  = speed of light.

### 3. Gaussian Beams and Hermite-Gaussian Mode Patterns

The intensity of the beam pattern when it exits the cavity is stronger in the center. Any mode of a laser represents a self-reproducing field which does not change shape from pass to pass between the mirrors. The beam shapes satisfying this fundamental requirement are the Hermite-Gaussian modes. The simplest transverse electromagnetic mode has a Gaussian intensity profile. The size of the laser cavity and the exit aperture control these modes (Siegman,1986). The Synrad laser has 98% of the energy in  $TEM_{00}$ . The diameter or spot size will depend of the distance traveled (Harney,1996):

$$w^2(z) = w_0^2 \left[ 1 + \left( \frac{z}{z_0} \right)^2 \right] = w_0^2 + \frac{1}{4} \theta^2 z^2,$$

$\theta$  = Divergence angle,

$w_0$  = Beam waist.

#### 4. Safety

To prevent exposure to direct or scattered invisible laser radiation, the device provides indication and control of the radiation presence and warnings of the potential hazard. Safety glasses were used to reduce the risk of eye damage, and firebricks were used as external beam-blocks.

The equipment has panel controls and indicators, internal safety circuit elements, input/output interfaces, a keyswitch, a remote interlock on/off circuit, and a laser aperture shutter switch, a fault internal electronics and 60 degrees over temperature output signal, and the device has a 5-second delay between power and the onset of lasing.

#### 5. Technology and Operation

The beam shape is square at the laser output aperture, but it changes to approximately circular at a range of 1 m. The laser beam diverges due to diffraction at a full angle of 4 mrad, with the beam waist at the exit aperture. This laser uses a RF excitation method to stabilize the discharge. The RF drive frequency is 45 MHz to match the resonant frequency of the plasma tube. The Power control is continuous, fixed at +5VDC in this case, to cause the laser to operate in a CW mode (100% duty cycle).

The laser consists of a RF excited plasma tube with an adjustable mirror on each end, mounted together with the RF drive assembly in a single aluminum chassis. The plasma emission is formed only in the 4.8 mm<sup>2</sup> bore region.

The optical resonator consists of 3 m radius of curvature total reflector and a flat ZnSe output coupler with reflectivity of 95%. The 4.8 mm bore, and the mirror curvature, limits the output beam to TEM<sub>00</sub> modes, when the mirrors are aligned.

The DC power supply used provides 28 V for operation of the laser. Laser current is about 8 A. Typical efficiency of CO<sub>2</sub> laser plasma tubes operating at TEM<sub>00</sub> mode is 10 to 12%. At the 10 W laser power output level a considerable amount of heat (200 W) must be removed, applying air cooling in this case, using a cooling fans system. This system delivers 500 ft<sup>3</sup>/min of air.

## **E. OPTICS**

The primary purpose of the optical system is to split the beam to produce the reference and the beam that is going to the target, and then recombine the first one with the returning beam from the target. During the optical path to and from the target the beam is first expanded and collimated. The returned beam is focused. The optical system consists of a number of Melles Griot lenses, beamsplitters and mirrors.

### **1. Lenses**

Attenuation is wavelength and material dependent. The lenses used were chosen for minimum attenuation of the intensity of the light.

#### **a. Beam Expander**

This sub-system expands the laser light beam to the size of the target, after the acousto-optic modulation. It consists of:

(1) One ZnSe negative plano-concave lens, focal length  $-50\text{mm}$ ,  $25\text{mm}$  diameter, to cause the small beam spot to diverge.

(2) One ZnSe positive plano-convex lens, focal length  $+150\text{mm}$ ,  $25\text{mm}$  diameter. It is used to recollimate the beam and direct the expanded light spot to the retroreflector vibrational target.

#### **b. Beam Collector**

This directs both the reference and the target beam spots at the detector. It consists of: one ZnSe positive plano-convex lens, focal length  $+254\text{mm}$ ,  $25\text{mm}$  diameter. It is used to collect the coincident final spot on to the detector area.

### **2. Plate Beamsplitters**

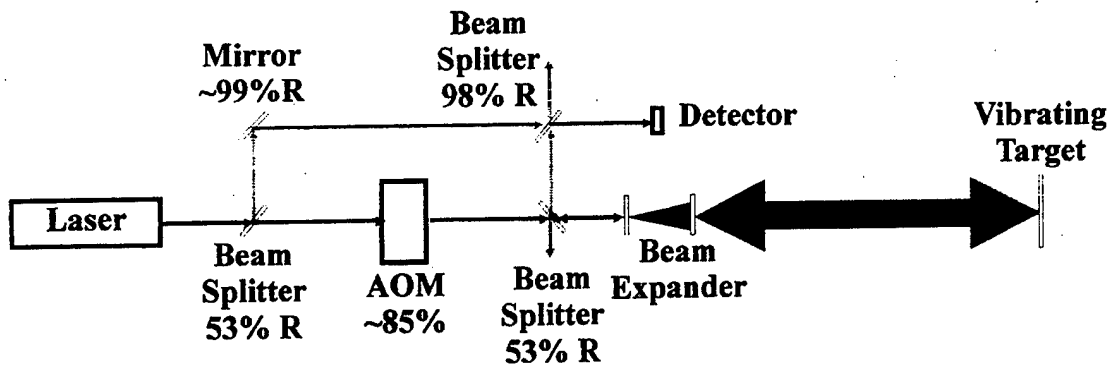
Beamsplitters separate the incident beam into two beams whose paths are 90 degrees apart, one portion of the beam is transmitted, and the other one is reflected. The beam splitting percentage (what fraction is reflected) is a function of polarization. The beamsplitter set consists of:

Two plate beamsplitters whose nominal reflectance/transmittance ratio is 50/50. Their diameters are  $25\text{mm}$ . They are used before the acousto-optic modulation to produce the reference beam and after the acousto-optic modulation to direct the modulated beam to the target, and then to the next sub-system, described below.

One plate beamsplitter whose nominal R/T ratio is 90/10, and whose diameter is  $25\text{mm}$ . This directs both the reference and the shifted beam to the beam collector described above, which finally directs both beams to the detector.

### 3. Mirrors

The optical system has one flat Si mirror, to direct the reference beam into the path of the target returned beam.



**Optical Transmitting Efficiency =  $(0.53)(0.85)(1 - 0.53) = .21$  or 21%**

**Optical Receiving Efficiency =  $(0.53)(0.98) = .52$  or 52%**

Fig.4 Optics sub-system configuration of the laser radar system.

## F. ACOUSTO-OPTIC SHIFT

The acousto-optic modulator (AOM) shifts the frequency of the transmitted light in the laser radar, producing a frequency shift between the target return and the reference. For this project an IntraAction Corp infrared AOM/Frequency Shifter, model AGM-406B1 was used. It works at 10.6  $\mu\text{m}$  wavelength. It is comprised of a germanium optical single crystal, and produces an optical frequency shift in the range of +/- (30 to 50 MHz).

### 1. Acousto-optic Effect

When the germanium medium is subjected to compressive and refractive acoustic pressure waves, its refractive index will change as result of the mechanical strain. The amount of change is proportional to the square root of the total acoustic power applied (Wilson,1989). For this case the Ge crystal is transparent to the incident 10.6  $\mu\text{m}$  incident light, which is going to be affected by the change of the material's index of refraction. The areas of low pressure and low refractive index will allow the light to pass through faster. High-pressure areas will slow the incident light down (Wilson,1989).

If the incident light crosses the medium in a direction perpendicular to the acoustic waves, a modulated optical wave front will result. A standing acoustic wave in the medium will create a diffraction grating with a ruling spacing determined by the acoustic wavelength. We use the crystal in a travelling wave configuration

### 2. The Bragg Regime

In this case the medium is thick, in order to modulate the frequency of the incident light. In this regime the diffraction is complete and the acoustic field acts like a succession of planes of traveling mirrors. These traveling acoustic wave fronts reflect the incident light. Under appropriate conditions, the light that is reflected off of successive traveling mirrors arrives in phase at the new reflected wavefront. For this to occur, the path differences between the successive reflections off of the travelling mirrors must be an integer number of wavelengths. To accomplish this condition the incident light must have a specific Bragg angle (Wilson,1989):

$$\theta_B = \sin^{-1} \left( \frac{m\lambda}{2\Lambda} \right),$$

$m =$  Order of diffraction,

$\Lambda =$  Acoustic wavelength,

$\lambda =$  Wavelength of the incident light.

An acoustic damper at the end of the AOM allows acoustic waves to travel only in one direction across the medium. Incident light that is reflected off of these planes is going to be Doppler shifted (Wilson,1989):

$$\Delta\nu = \frac{\pm 2n_m V_a \sin\theta_B}{\lambda},$$

$V_a$  = Acoustic velocity,

$n_m$  = Refractive index of medium.

Then the modulation shift or acoustic wave frequency is:

$$f_s = \pm \frac{V_a}{\Lambda}.$$

The signs mean that the frequency can be up or down-shifted, depending on the orientation of the AOM, or the direction of the traveling acoustic waves.

An IntraAction Corp. RF Modulator Driver model GE-3030 drives the piezoelectric acoustic wave generator of the AOM. This power source provides the acoustic signal at a frequency of 30 MHz. The maximum power intensity of the reflected light is dependent on the diffraction efficiency, which is 85% in this case.

## **G. TARGET**

The configuration of this laboratory target allows us to control its frequency and amplitude of vibration. The target consists of an optical retroreflector mirror bonded to a vibrating piezoelectric actuator. The bond between the retroreflector and the piezoelectric actuator frequently broke due to vibrational fatigue and required rebonding with epoxy adhesive.

### **1. Retroreflector**

An Edmund Scientific broadband Al-SiO<sub>2</sub> retroreflector model C43652 was used. It produces no polarization rotation in the IR input beam, and has a parallelism of 1 arcsec, good thermal stability, and a mass of 32 grams.

The retroreflector is constructed of three optically flat, front-surface mirrors assembled into a corner cube. This geometry results in a reflected optical beam which is precisely parallel to the incident beam independent of reflector orientation.

### **2. Piezoelectric Actuator**

The piezoelectric actuator is a ThorLabs actuator PE4. Its mass is 4.8 grams, and it allows a maximum of 17.4  $\mu\text{m}$  displacement when driven by a ThorLabs low noise single channel piezo driver model MDT691.

The resonant frequency of the actuator is affected by the resonant frequency of the total piezoelectric target configuration. The resultant resonant frequency is 18KHz. The fastest response time of the system is 18.5  $\mu\text{sec}$ . The maximum frequency achieved without damaging the actuator is related to the actuator limiting strength and the maximum vibration amplitude. For a 1  $\mu\text{m}$  minimum amplitude displacement the maximum frequency is 4,600 Hz. For 17.4  $\mu\text{m}$  maximum amplitude the minimum frequency is 1,100 Hz.

The actuator's capacitance limits the target bandwidth. Because the sinusoidal signal generator that creates the sinusoidal displacement is not electrically matched to the actuator, the drive signal goes through the ThorLabs amplifier model MDT691, which supplies the 60 mA required for the actuator.

The amplifier allows the target to receive up to 150V, resulting in 17.4  $\mu\text{m}$  maximum displacement, at a maximum frequency of 143 Hz. At the smaller amplitude of 1  $\mu\text{m}$  the maximum achieved target vibration frequency is 2,485 Hz.

## H. DETECTOR

The detector houses a 1 mm<sup>2</sup> HgCdTe room temperature photoconductive element with an antireflection coated germanium window. It has 60 degree field of view, detectivity of  $6.1 \times 10^{10}$  cm/W $\sqrt{\text{Hz}}$  at 1KHz, and peak wavelength 10.6  $\mu\text{m}$ . The detector noise level is 3 nV/ $\sqrt{\text{Hz}}$ .

The incident laser light photon energy raises electrons into the conduction band of the detector. The minimum required photon energy to do this is related to the wavelength and the energy band gap of the detector (Wilson,1989):

$$\lambda = \frac{hc}{E_g}.$$

$E_g = \text{Energy band gap.}$

When photons of the right wavelengths strike the detector, its conductivity increases. The detector noise level is due to the fluctuations in the generation and recombination rates of electron-hole pairs, and the thermal generation noise that occurs at the room temperature.

The noise equivalent power (NEP), is a measure of detector noise. It is the applied signal power which produces a signal voltage just equal to the rms noise voltage, as represented in the following equation(Wilson,1989):

$$NEP = \frac{(A_d \Delta f)^{\frac{1}{2}}}{D^*},$$

$A_d = \text{Detector area,}$   
 $\Delta f = \text{Frequency bandwidth.}$

The detectivity ( $D^*$ ) is another parameter characterizing the relationship between signal-to-noise ratio and applied signal power. It depends on the detector area and the frequency bandwidth, as in the following equation (Schlessinger,1995):

$$D^* = \frac{(A_d \Delta f)^{\frac{1}{2}}}{P} \left( \frac{V_s}{V_n} \right),$$

$P = \text{Incident power,}$   
 $\frac{V_s}{V_n} = \text{Voltage signal - to - noise ratio.}$

The detector responsivity (R) measures the ratio of the detector output versus the incident optical power. In this case it is equal to 100 mV/W. The carrier-to-noise ratio (CNR) determines how much incoming signal is needed to achieve detection at a level greater than the detector noise. It depends of the detector quantum efficiency (the ability

to convert photons into current). The CNR is also affected by the local oscillator beam noise. For heterodyne detection (Jelalian, 1992):

$$\text{CNR} = \frac{\eta_D P_{LO} P_{\text{signal}}}{hfB (P_{LO} + P_{\text{signal}} + P_{BK}) + \sum K P_{\text{noise}}},$$

$\eta_D$  = Detector quantum efficiency,

$B$  = Electronic bandwidth,

$P_{\text{signal}}$  = Received signal power,

$P_{LO}$  = Local oscillator power.

If the reference beam is very strong, it will dominate the noise terms, simplifying the equation:

$$\text{CNR} = \frac{\eta_D P_{\text{signal}}}{hfB}.$$

## I. SIGNAL PROCESSING ELECTRONICS

The electronics circuitry takes the signal coming from the detector, and transforms it into an amplitude-modulated voltage. This will be further processed by the signal analyzer system, which displays the resultant signal in the frequency domain.

To accomplish this, the detector signal is amplified and transformed into a voltage signal using a Melles Griot high frequency amplifier model 13AMP007. It provides a transimpedance gain of 6,250 V/A over a frequency range of 4 kHz to 400 MHz, and the operating bias voltage needed by the detector.

To restrict the frequency range and to reduce the noise, after the amplifier the signal is passed through a limiter and a frequency discriminator circuit, with high, low and band pass filters between them.

### 1. Filters

Low pass filters Mini-Circuit SLP-50: -3dB passband from 0 to 50 MHz. High pass filters Mini-Circuit SHP-25: -3dB attenuation point of 25 MHz. Band pass filters Mini-Circuit SBP-30: centered at 30 MHz with elliptical response 3 dB bandwidth of 10 MHz. Together each set of three filters eliminates all noise outside of a passband from 25 MHz to 35 MHz.

## 2. Limiter Miteq Model LCPM-30/10-70B

The input signal can fluctuate wildly in amplitude. To help to stabilize the fluctuations in signal amplitude, which cause variations that the frequency discriminator which can translate into distorted frequency readings, a limiter is used. The limiter also acts as an amplifier: signal inputs ranging from  $-65$  to  $5$  dBm are amplified by the limiter to a constant  $10.74$  dBm. The frequency range is centered on  $30$  MHz with bandwidth of  $20.9$  MHz.

## 3. Frequency discriminator Miteq model FMDM-30/6-8B

The frequency discriminator converts frequency modulation in the signal into simple amplitude modulation.

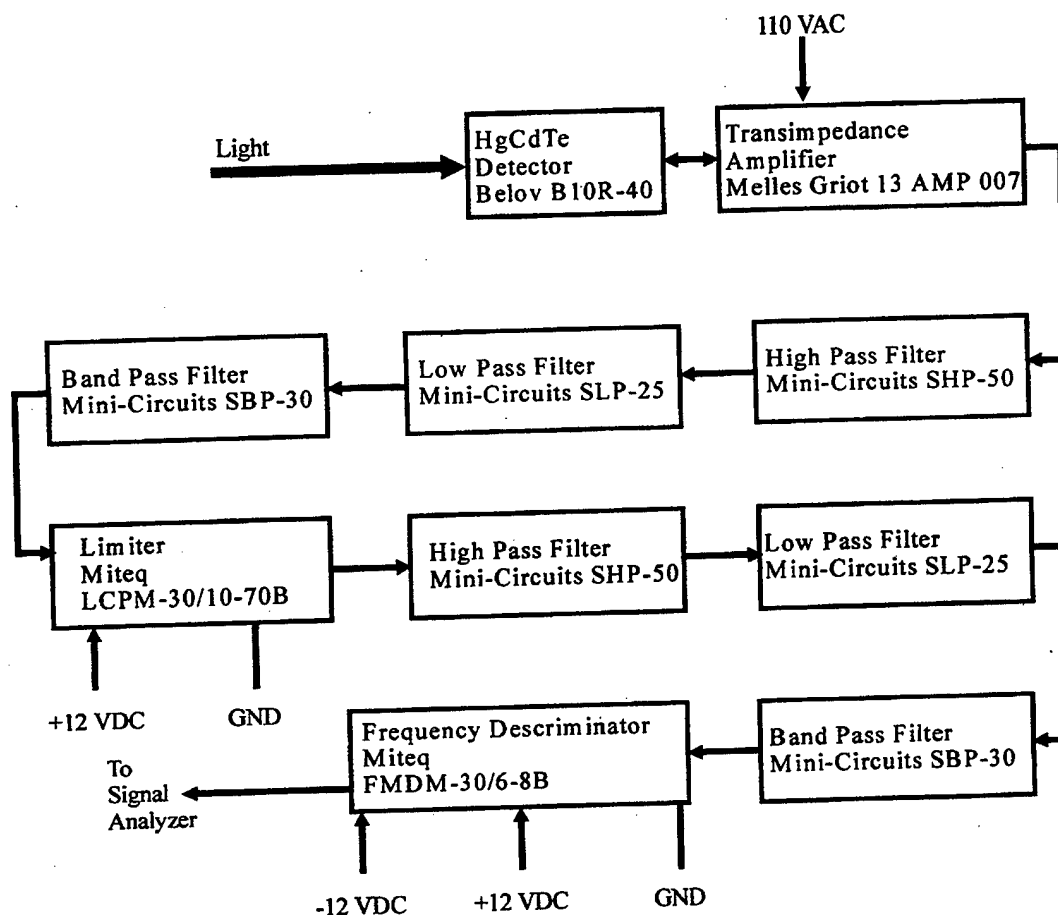


Fig.5 Signal processing electronic circuitry of the detector sub-system.

### III. DATA ACQUISITION

The data acquisition process has three elements: data acquisition, data analysis, and data presentation. The data acquisition is obtained using a plug-in device, the data analysis transforms the data into meaningful information, using the programs available, and the data presentation tool allows effective communication with the system, using a graphical user interface.

#### A. VIRTUAL INSTRUMENT

The addition of a virtual instrument (VI) to the laser radar hardware, a virtual spectrum signal analyzer, was the main task of this project, permitting the performance of the laser radar to be increased. This requires interface hardware, the DAQ card PC-516, and functional software LabView; it makes the use of the previously employed real instrument unnecessary. With the VI, the expansion of the project is functional and flexible, because the instrumentation system can be upgraded or changed entirely in software. The high-performance virtual instrument allows the computer display to present the measurements, providing processing and data memory.

The LabView software is an important piece in the system, providing the tools to design virtual instruments, and make use of all the possible applications. VI libraries are available, making the development time shorter. The code is easy to learn and self-helping, with many troubleshooting utilities (Johnson,1994). In addition to signal processing and display, LabView also provides the signal source for the laser radar.

The system functionality was defined by the performance of the computations on the data. The LabView software is a graphical programming language that interacts with Windows 95.

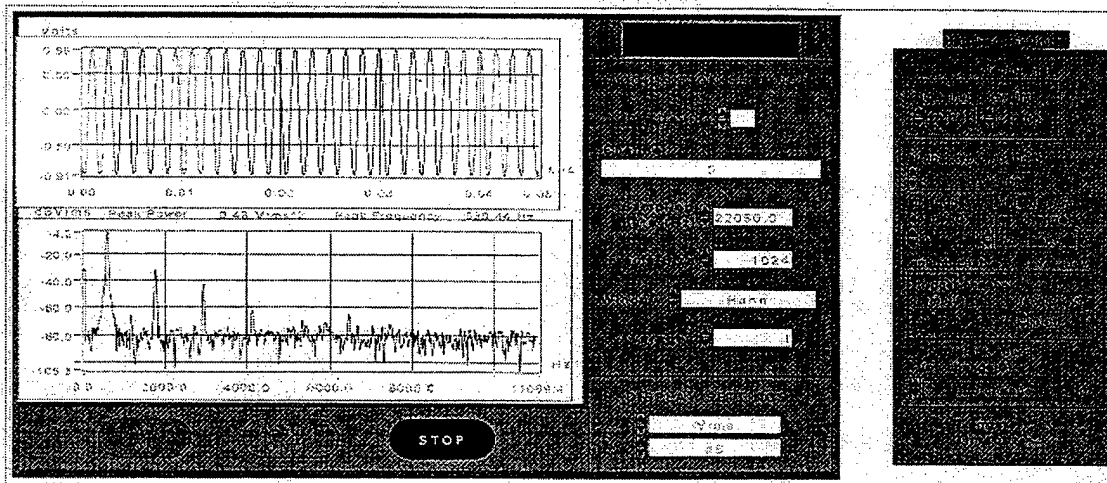


Fig.6 The Virtual Benchtop spectrum analyzer as seen on the computer display.

The ready-to-run instrument is named as a Spectrum Analyzer VirtualBench Instrument. The VI spectrum analyzer is a digital sampling instrument that uses fast Fourier transform (FFT) techniques to analyze low frequency signals in the vibration field.

The VI Spectrum Analyzer application has three components: acquisition and control, data analysis, and data presentation.

The VirtualBench instrument permits the acquisition and saving of waveform data to computer memories and disks, and has a post-report and printing generation capability. With this it's possible to print the waveforms and the settings of the instrument at any time.

The characteristics of the virtual instrument are summarized as follows:

- Bandwidth: DC to 20 kHz,
- Sampling rate: 51.2 ksamples/sec,
- Dynamic range: 93 dB with alias protection,
- Precision: 16-bit ADC with sampling,
- Amplitude flatness: +/- 0.025 dB,
- Analog input: Up to 2 channels,
- Analog output: One precision A/O,
- Frequency resolution 1: 850-line (0.025 dB bandwidth),
- Frequency resolution 2: 920-line (3 dB bandwidth),
- Cursors: Delta-t and Delta-y measurements,
- Measures: Total harmonic distortion (THD), harmonic contents, frequency response, power spectrum, amplitude spectrum, coherence, and cross spectrum.
- Record lengths: Up to 2,048 points,
- Trigger modes: Analog and digital,
- Waveforms can be saved to computer memory or disks,
- Capacity to print hard copies of waveforms and settings.

This virtual instrument measures total harmonic distortion, harmonic content, frequency response, impulse response, power spectrum, amplitude spectrum, coherence, and cross power spectrum. Built-in windowing functions include Hanning, Flat top, Hamming, Blackman-Harris, Blackman, and Exact Blackman to reduce the effects of aliasing.

The virtual instrument display functions as a low frequency oscilloscope to view signals in the time and frequency domains simultaneously. It displays two different traces at the same time. The upper trace is the time domain waveform graph of the signal, expressed in volts versus seconds. The lower trace is the frequency domain or power spectrum of the signal, expressed in dBm versus frequency. Cursors facilitate extraction of key control system performance parameters, such as overshoot, rise time, settling time, and delay time.

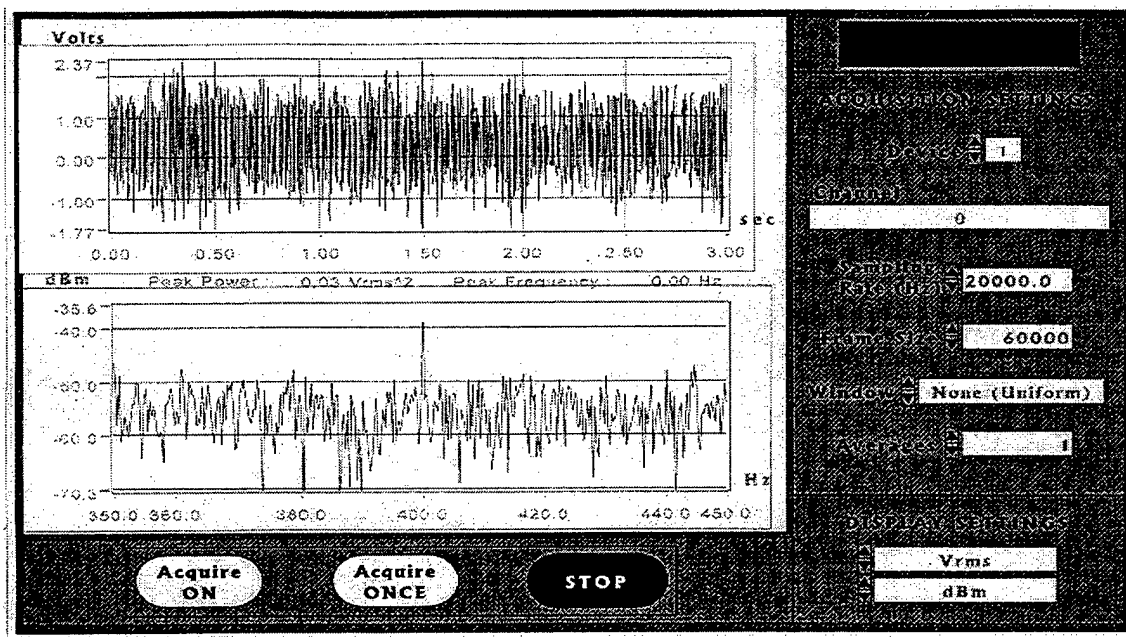


Fig.7 VI spectrum analyzer showing the target vibrating frequency peak at 400 Hz.

## B. HARDWARE

The plug-in board National Instruments PC-516 represents the brain of the VI. It has analog, digital and timing I/Os, programmable channels, sampling and conversion modes, separate gain for each channel, delayed, analog, and digital triggering.

### 1. Characteristics

- Fast instrumentation implementation and performance,
- Plug and play device,
- Transfers data to and from the computer memory,
- 8 to 16-bit resolution,
- Sampling rates up to 1 MHz,
- Analog-to-digital (A/D) and digital-to-analog (D/A) conversions,
- Digital I/O,
- Advanced counter/timers operations: 03,
- Portable interfaces: PC cards for portable computers,
- High performance,
- Fast settling time,
- High accuracy,
- Multiboard synchronization,
- Shielded I/O connectors,
- Portability: 4.25x4.3 in.,

- Operating temperature: 0 to 70 °C.

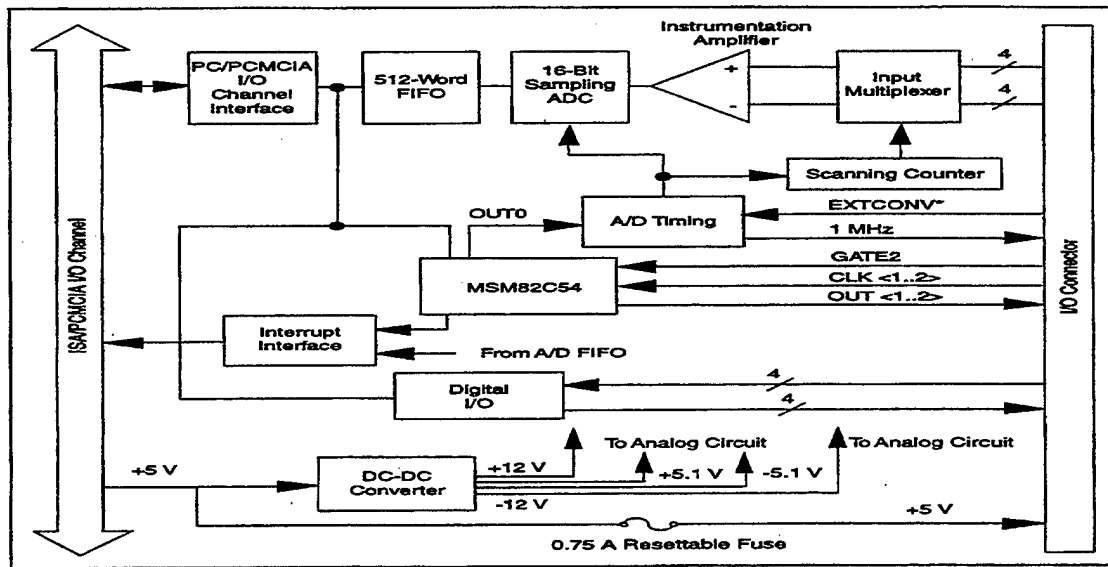


Fig.8 National Instruments PC-516 data acquisition card block diagram.

## 2. Multifunction I/O

The PC-516 is a plug-and-play compatible, analog input, digital I/O, and counter/timer board for PC-compatible computers. It has a 16-bit, successive-approximation ADC with eight single-ended analog inputs or four differential inputs, a 4-bit TTL-compatible digital input port, a 4-bit TTL-compatible digital output port, and two user-available 16-bit counter/timer channels for counting and timing I/O, and frequency measurements. The card is configured and calibrated entirely by software (National Instruments, DAQ, PC-516 User Manual, 1996).

The input circuitry has input overvoltage protection of  $\pm 25$  V powered on or powered off, and the voltage input range is  $\pm 5$  V. The ADC performs 20  $\mu$ s conversions with single-channel and multichannel, aggregates acquisition sampling rates up to 50 kS/s. Continuous data acquisition mode was used.

The most important application that it has is signal analysis. Implementation of that application is the purpose of this thesis project. The device is connected to the laser radar through a connector built by the student.

## 3. Card Software

The card was provided with the NI-DAQ National Instruments DAQ driver, that manages all functions of the hardware, and lets an application be started without having to program the card. The LabView application software can also be used to program the hardware. Both programs have extensive libraries for data acquisition, instrument control,

data analysis, and graphical data presentation (National Instruments, DAQ, PC-516 User manual, 1996). The software supports the following operations:

- Analog input (A/D conversion),
- Buffered data acquisition ( high-speed A/D conversion),
- Analog output (D/A conversion),
- Waveform generation,
- Digital I/O,
- Counter/timer operations,
- Self-calibration,
- Messaging,
- Acquiring data to extended memory.

#### **4. Cabling**

For the purpose of this project no cable termination accessory was used. The signal input and output wires are attached to a handmade terminal, and there is no connector block.

To connect the card a standard 30-conductor ribbon cable was used with a polarized, 30 pin, insulation displacement, male ribbon cable header connector at one end. According to the pin assignment for the connector the appropriate analog input channel (ACH1) was connected to the signal, coming from the radar, and the analog input ground (AIGND) was connected to the radar ground.

#### **5. Configuration**

Taking into account measures to prevent electrostatic discharge damage to the board, it was installed by the student in a 16-bit expansion slot in the PC, following the instructions from the user manual. Two types of configuration were performed on the board: bus-related and data acquisition-related. The first one includes setting the I/O address. The second one includes analog input mode, digital I/O configuration, and counter configuration (National Instruments, DAQ, PC-516 User manual, 1996).

The analog input mode was the referenced single-ended (RSE) input. RSE input means that all input signals are referenced to a common ground point that is also tied to the device analog input ground. This configuration is useful for measuring floating signal sources, and can monitor eight different analog input channels.

Single-ended connections are those in which all PC-516 device analog input signals are referenced to a common ground. The input signal is tied to the positive input of the instrumentation amplifier that is referenced to their common ground point. To make this connection, the input signal met these criteria:

- The input signal is high level (greater than 1 V),
- Leads connecting the signal to the PC-516 device are less than 15 ft. long,
- All inputs signals share a common reference signal (at the source).

A ground-referenced signal source is connected to the building system ground, like the laser radar device that is being used. The difference in ground potential between two instruments connected to the same building power system is typically between 1 and 100 mV, and because of this, the ground-induced noise is negligible.

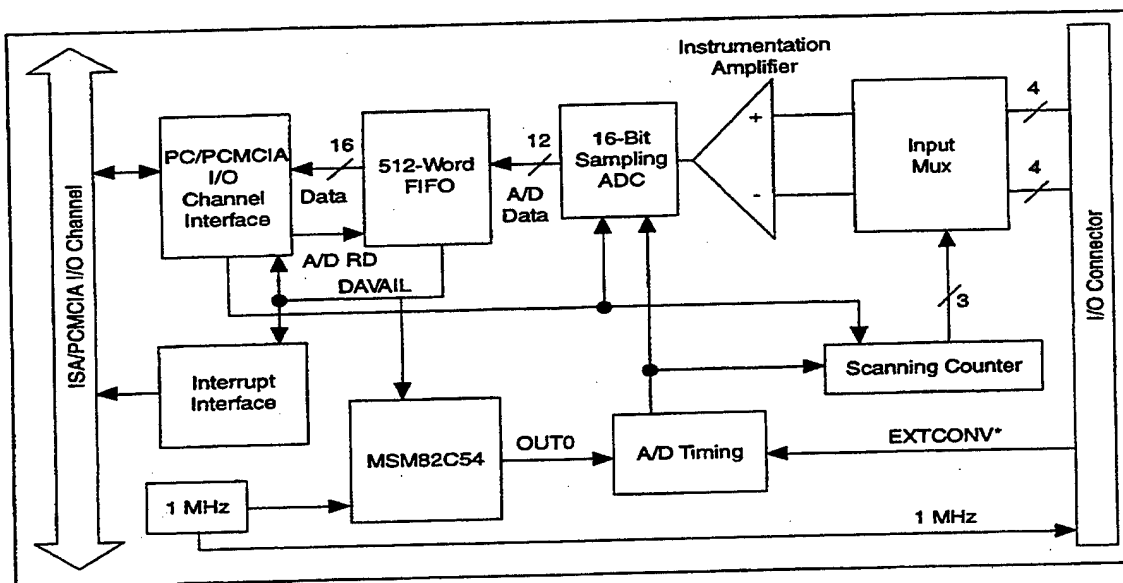


Fig.9 Analog input and data acquisition circuitry block diagram.

The principal components of the device are:

- Bus interface circuitry,
- Analog input circuitry,
- Digital I/O circuitry,
- Timing I/O circuitry.

The data acquisition functions are executed by the analog input circuitry and some of the timing I/O circuitry. The internal data and control buses interconnect the components. A data acquisition operation refers to the process of obtaining a series of successive A/D conversions at a carefully timed interval. This interval is called the sample interval.

During single-channel data acquisition, a control register selects the analog input channel before data acquisition starts. These multiplexer settings remain constant during the entire data acquisition process; therefore, all A/D conversion data is read from a single channel.

## **C. SOFTWARE**

### **1. LabView**

LabView is graphical programming software. This software permits instrumentation, data analysis, simulation, control, and measurement, in this case, a vibration analysis application (National Instruments, LabView, User manual, 1996).

One of the features of this software is that, it can be adapted to different operator skill levels. Performance of the system is improved by integrating the application software, with the device driver software and hardware.

LabView is the medium for integrating the virtual instrument into a standard computer, and gives the capability of data acquisition, data analysis and data presentation. For this thesis research, the measure and virtual Bench library adds easy-to-use non-programming solutions for data acquisition, which results in the virtual spectrum analyzer. A LabView program has three principal elements:

- The application,
- The measurement program, and
- The instrument driver.

This instrument driver can be called from the block diagram available for the virtual instrument.

### **2. NI-DAQ Data Acquisition Software**

The DAQ hardware needs the NI-DAQ driver software. This software directly programs the registers of the hardware, managing operation and integration with the PC (National Instruments, DAQ, User manual, 1996). This software is an easy-to-understand interface. It has three important functions to control the hardware: analog I/O, digital I/O, and timing I/O.

The software can perform the following tasks:

- Acquires data at specified sampling rates,
- Acquires data in the background while processing,
- Uses programmed I/O, interrupts, and direct memory access (DMA) to transfer data,
- Streams data to and from disk,
- Performs several functions simultaneously,
- Integrates more than one DAQ board,
- Integrates with signal conditioning equipment.

With NI-DAQ software, it's possible to use and reuse the buffer continuously. As interrupts and DMA operations place data from the board into the buffer, the LabView application program pulls data out of the buffer for processing, saving to disk or upgrading screen graphics. When the buffer is full, the interrupt or DMA operation reinitializes its address pointer to the beginning of the buffer. In this way, continuous data

collection and processing can be sustained indefinitely, provided that the aforementioned maximum data sampling rate is not exceeded.

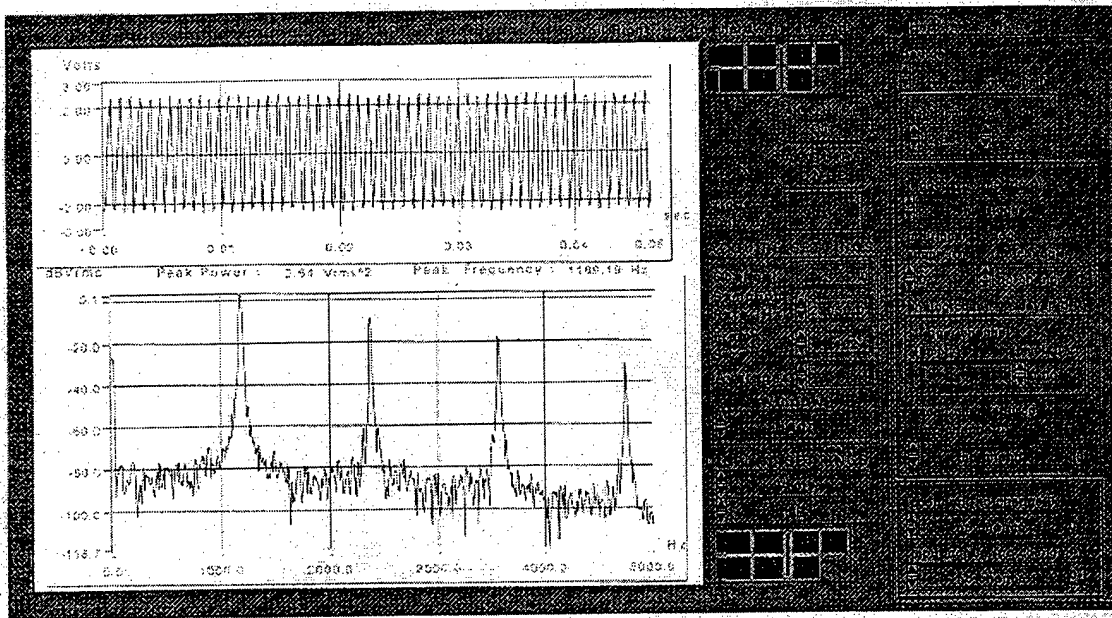


Fig.10 Virtual spectrum analyzer front panel as seen on the computer screen.

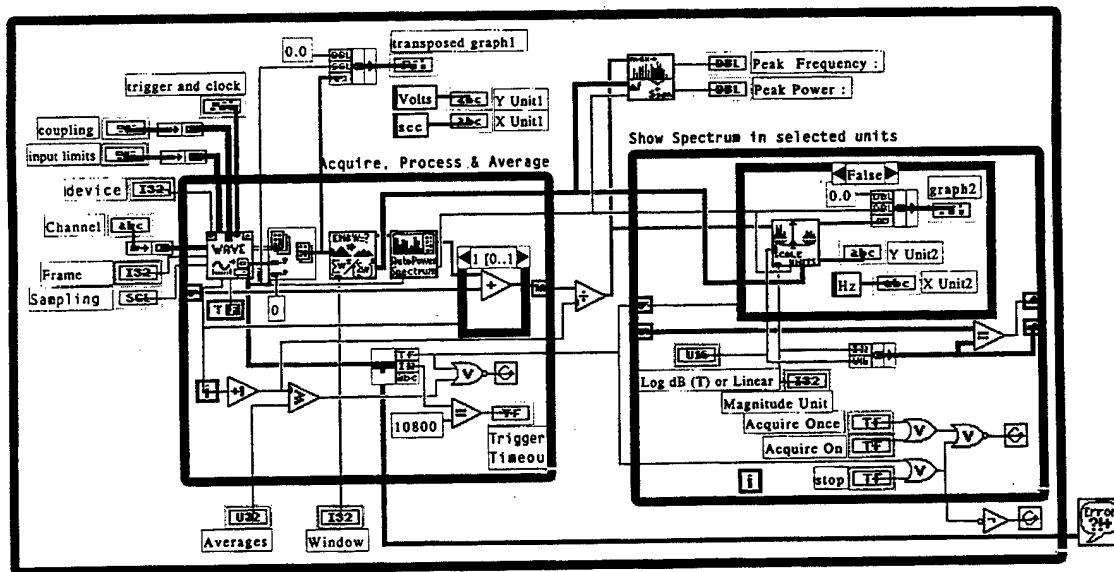


Fig.11 Virtual spectrum analyzer block diagram showing the sub-VI components.

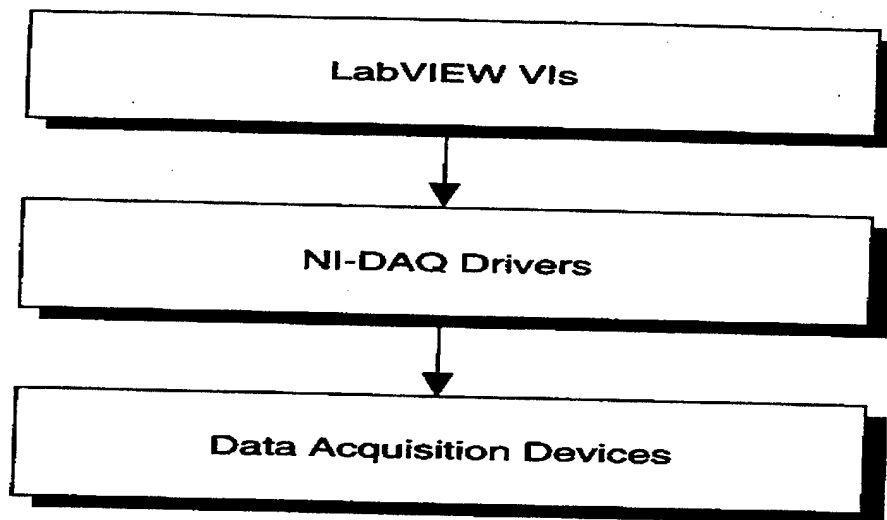


Fig.12 The data acquisition system is related to NI-DAQ and the DAQ Devices.



#### **IV. EXPERIMENTAL SET UP**

This section covers the set up of the laboratory, laser radar and computer-based measuring equipment. To begin this project the first thing that I did was to establish the main task to do: add a computer-based data acquisition and analysis system to improve the analog signal processing capability of the laser radar already designed and constructed (Day,1997).

The second thing was to obtain the required laser hazard evaluation and certification for class IV standard laser operation, from the NPS laser system safety officer, with the previous medical eye examination, and verification of the properly safety measures, to avoid any hazardous effect.

The third thing was to set up the computer, install the DAQ card and the software, connection of the computer to the laser radar, and familiarization with the software application.

The fourth thing was to set up and check the laser radar hardware and familiarization with its operational settings and emergency shut off procedure, including verification of the interlock switch. That includes verification of all electrical connections and power supplies.

##### **A. LASER RADAR SET UP AND OPERATING PROCEDURES**

The next thing to do was to verify the laser radar operational settings as follow:

1. To power the laser a 28 VDC power supply is used, in conjunction with a 5 V voltage source to control the lasing action.
2. Pre-operation: laser key switch off, power supplies off.
3. Stand-by: laser power supply on, laser key switch on, and control power supply off.
4. Operational: laser on (28 VDC, 5.36 Amp), control power supply on, air cooling system on.
5. Steady state: AOM water cooling system on, AOM power supply on, detector amplifier (+8V bias voltage) and electronic circuitry on, target signal generator and power supply on, computer on, virtual instrument running and real instrument on.

Once the laser radar is in steady state operation, the next thing to do was to check the correct optical alignment of the system, including the verification of the proper functioning of the AOM providing the frequency shift to the laser beam, and the correct

direction of the shifted and the unshifted beam from the AOM. A spatial filter, to avoid propagation outside the system, must correctly block the latter one.

The optical alignment of the system was the next critical step. It was accomplished by observing the output beams, using special IR beam probes, and their required UV lamp. It is necessary to adjust the optical system components to get the maximum intensity of the beam at the detector, adjusting first the local oscillator beam and then the returned beam from the target. The goal in aligning the reference and the target beam was to make them as parallel as possible and coincident, in order to obtain the correct interference at the detector. It was difficult to know exactly when the beam pointed directly into the detector element. To remedy this, the design of the detector mount was modified by the student, making it possible to move the detector in three dimensions to exactly adjust the position of the detector element at certain location to obtain the best heterodyne signal. Adjustments were always necessary at the start of each day's work.

The next step was to verify the laser power arriving at the detector and the target, using the available portable power meters. After the optical alignment, it was necessary to verify the retroreflector target performance, adjusting it to the desired vibrational frequency. The next step was to verify the proper work of the detector amplifier ( at +8V bias voltage) and the electronic circuitry. The analog electronics were repackaged by the student to make them less dependent on borrowed power supplies and more portable.

The last step was to verify the proper work of the virtual instrument on the computer, and the real instrument. Both were connected to the output signal from the laser radar, to have the spectral response from both displayed at the same time. Familiarization with the data acquisition software was needed, including a tutorial course done by the student and the reading of the manuals and bibliography available (National Instruments, Labview user manual, 1996).

To obtain the frequency spectrum data records, it was necessary to print from the real instrument, for comparison with the data obtained from the virtual instrument.

## V. OBSERVATIONS AND RESULTS

After all modifications and alignments to the laser radar were completed, a number of measurements were made to verify the performance of the new data acquisition and processing system. In the course of this verification a number of things were observed and several kinds of data were recorded. These are summarized below.

The laser radar is still able to detect vibrations from the target under laboratory conditions. The target vibrational frequency and amplitude were varied and the laser radar output was recorded. During the observations the target frequencies were 360, 380, 400, 420, and 440 Hz, making it possible to distinguish a shift of the vibration peak. The vibration amplitude in the target was changed between 40 nm to 1.7  $\mu\text{m}$ .

One of the interesting things during the experiment was the concern about the effect of the 60 Hz power line frequency interference and noise inside the resultant spectrum, and because of this, a sequence of tests was made.

First to all, the spectrum was measured while the system was totally off. For this case the 60 Hz pattern was observed with its respective harmonics, as shown in Fig 13. After this, the laser, detector and the electronics were turned on, leaving the AOM and target off. The result is that a big noise signature was detected inside the real time spectral response, as shown in the Fig. 14.

The next step was to add the AOM, and the result was that the 60 cycle pattern was still present in the spectrum. To reduce the noise, it was found to be necessary to average the signal response, as shown in Fig. 15. Both the real and the virtual instrument have the capability of averaging the signal.

When the target finally was turned on, vibrating at 400 Hz and 1.74  $\mu\text{m}$  amplitude, a very big peak response was observed at the target frequency, as shown in Fig. 16. For this case the signal was sampled at 50 ksamples/s and averaged 249 times. The 400 Hz peak is approximately 10 dB over the noise. There are other frequency responses that appear as well. Spikes also occur centered on the 400 Hz signal. These side bands appear intermittently throughout the duration of the experiment. Side bands of 60 Hz also appeared intermittently as well. Turning the target off makes the 400 Hz peak vanish.

There was an intermittent jump in the power spectrum occurring throughout the experiment. It was found that this jump is eliminated when the laser is off. This was observed with both real and virtual instruments. No source of this jump has been identified.

The spectral target responses at 360, 380, 400, 420 and 440 Hz, are shown in Fig. 17. Note the shift of the vibration peak from one frame to the next.

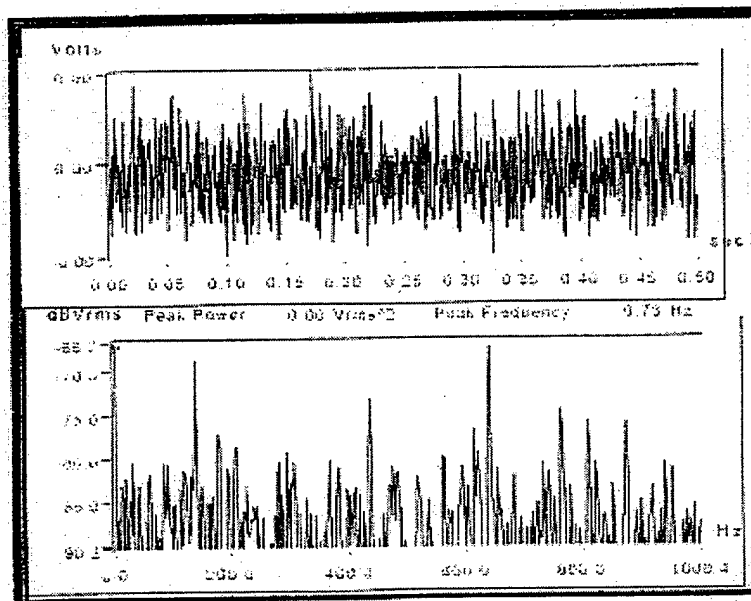
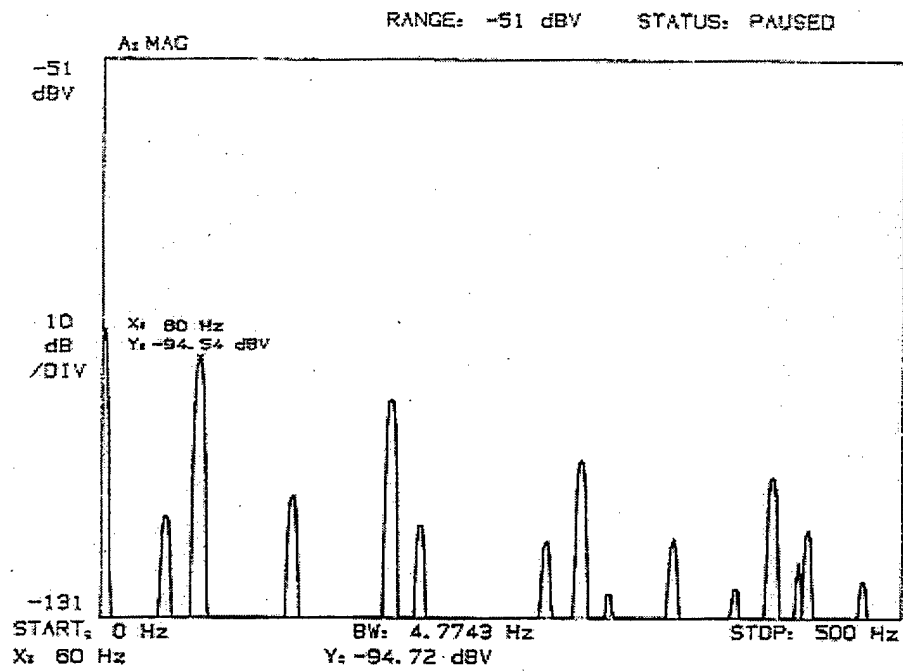


Fig. 13 Spectrum from the real and virtual instrument showing the 60 Hz pattern when the system is off.

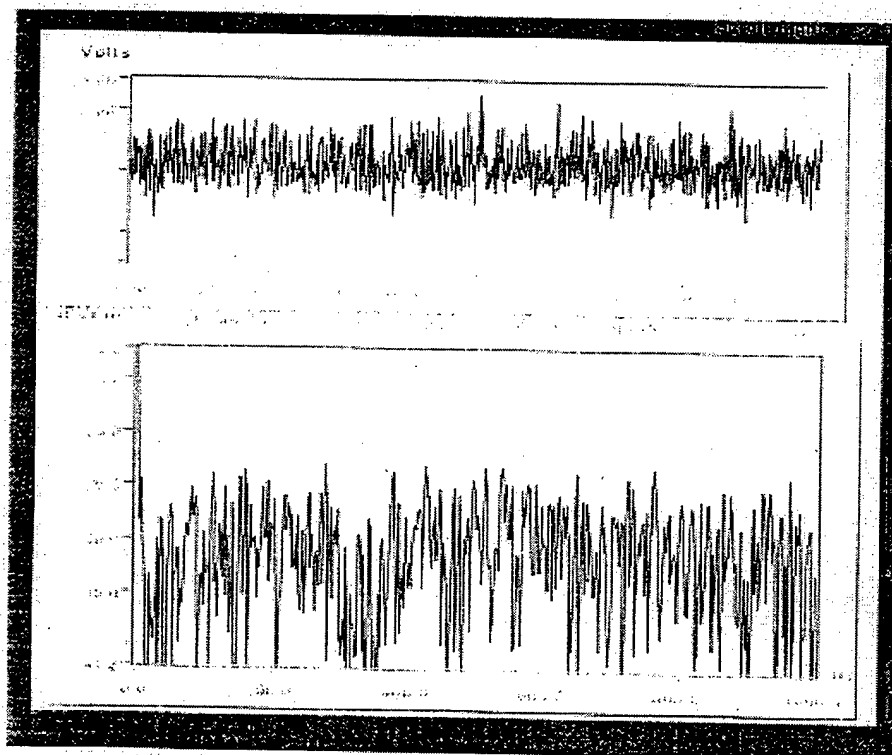
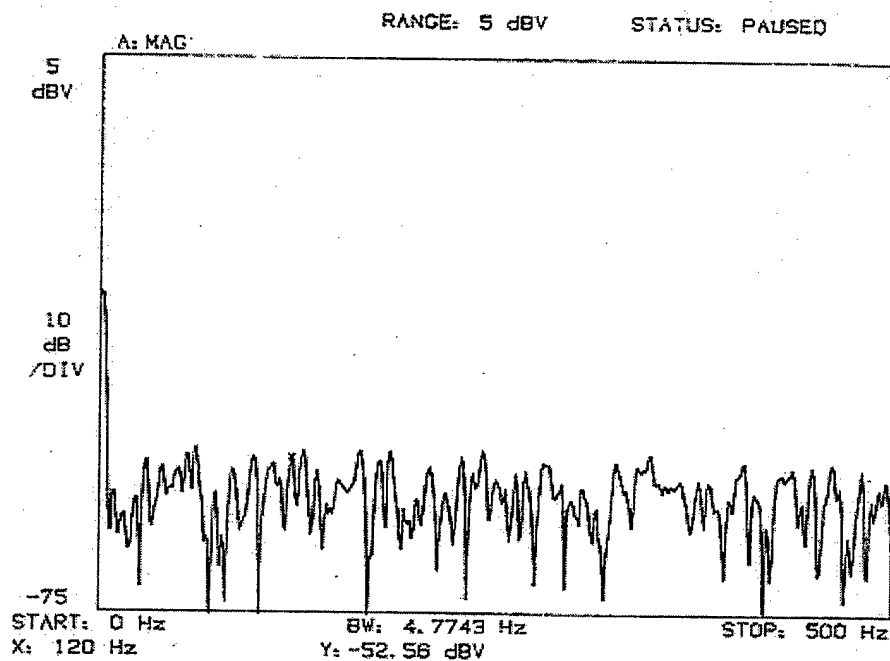


Fig. 14 Real time spectral response having laser, detector and electronic circuitry on.

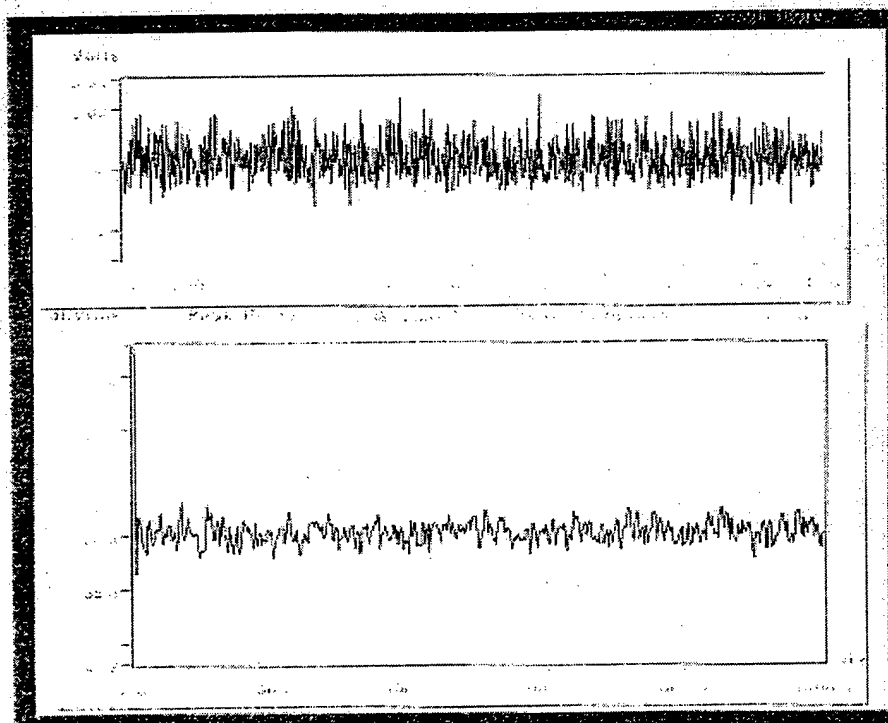
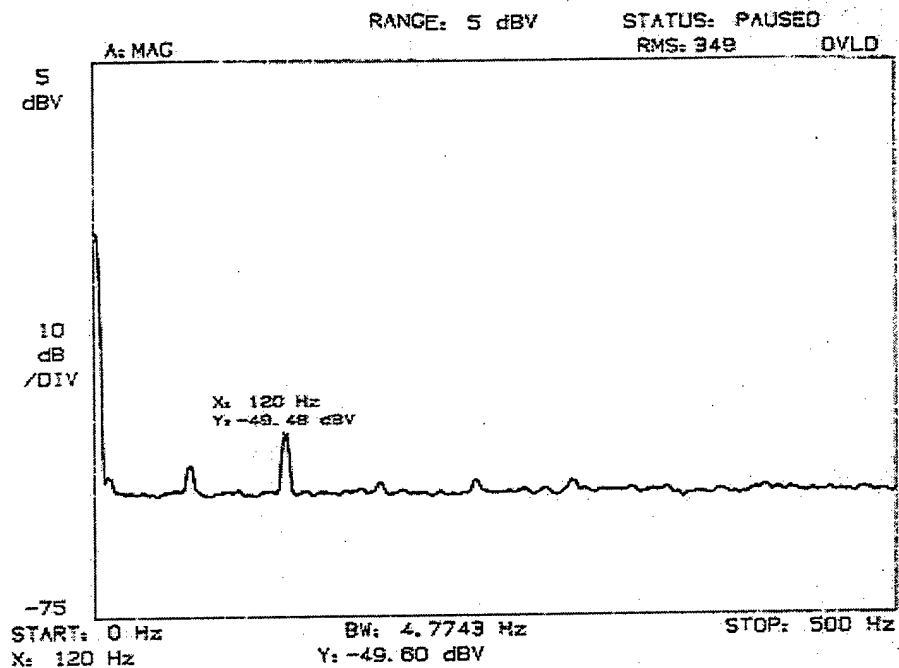


Fig.15 Averaged signal response having laser, detector, electronic circuitry and AOM on. Target vibration is off.

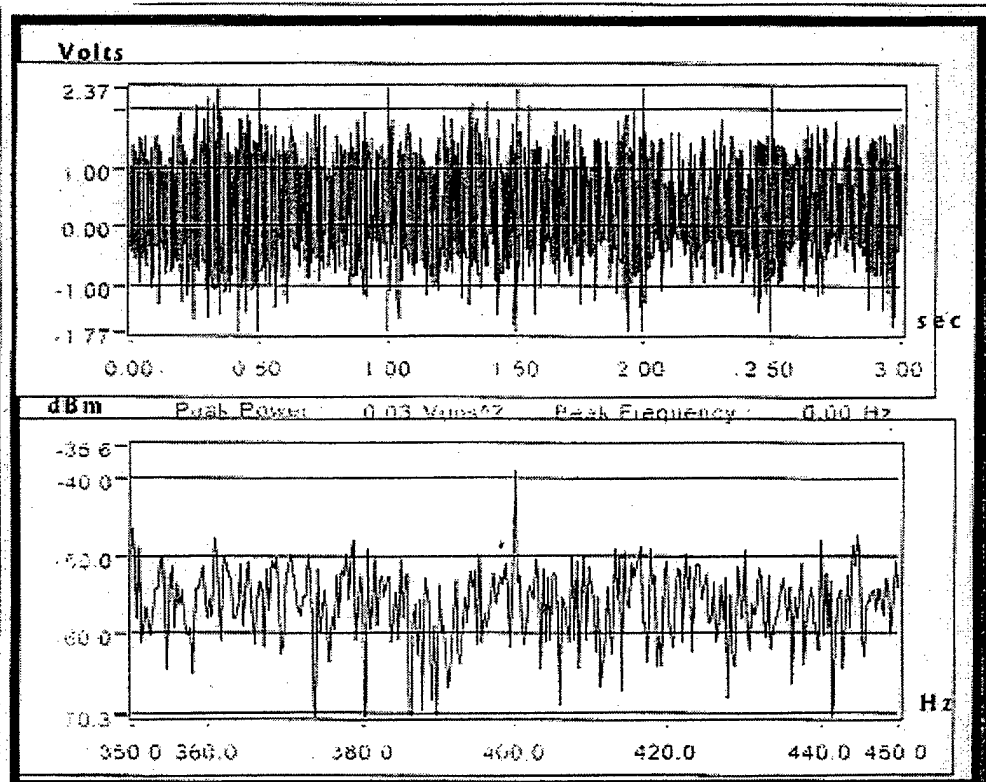
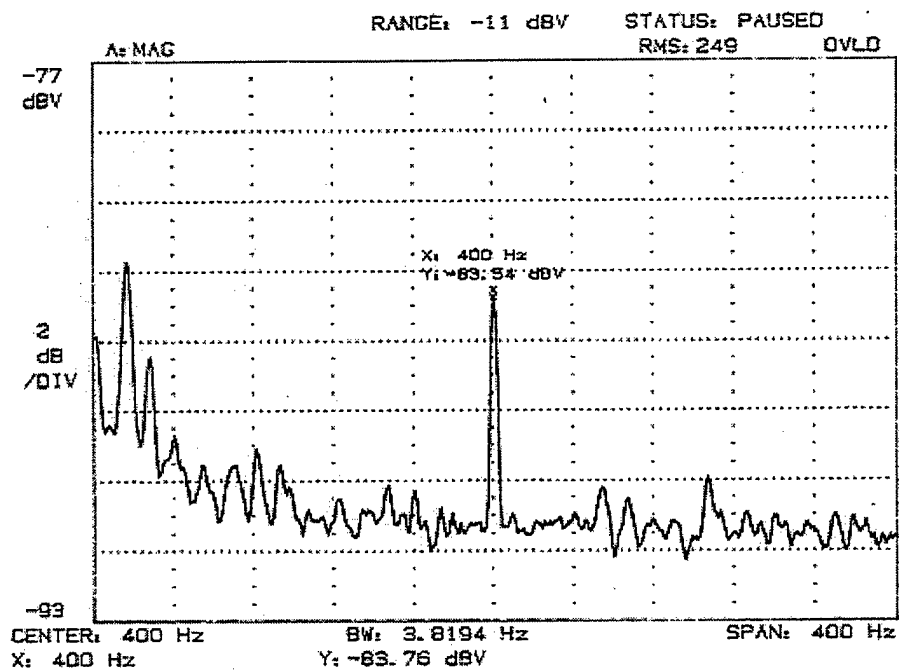


Fig. 16 Spectral response with the target on, at 400 Hz and 1.74  $\mu\text{m}$  amplitude.

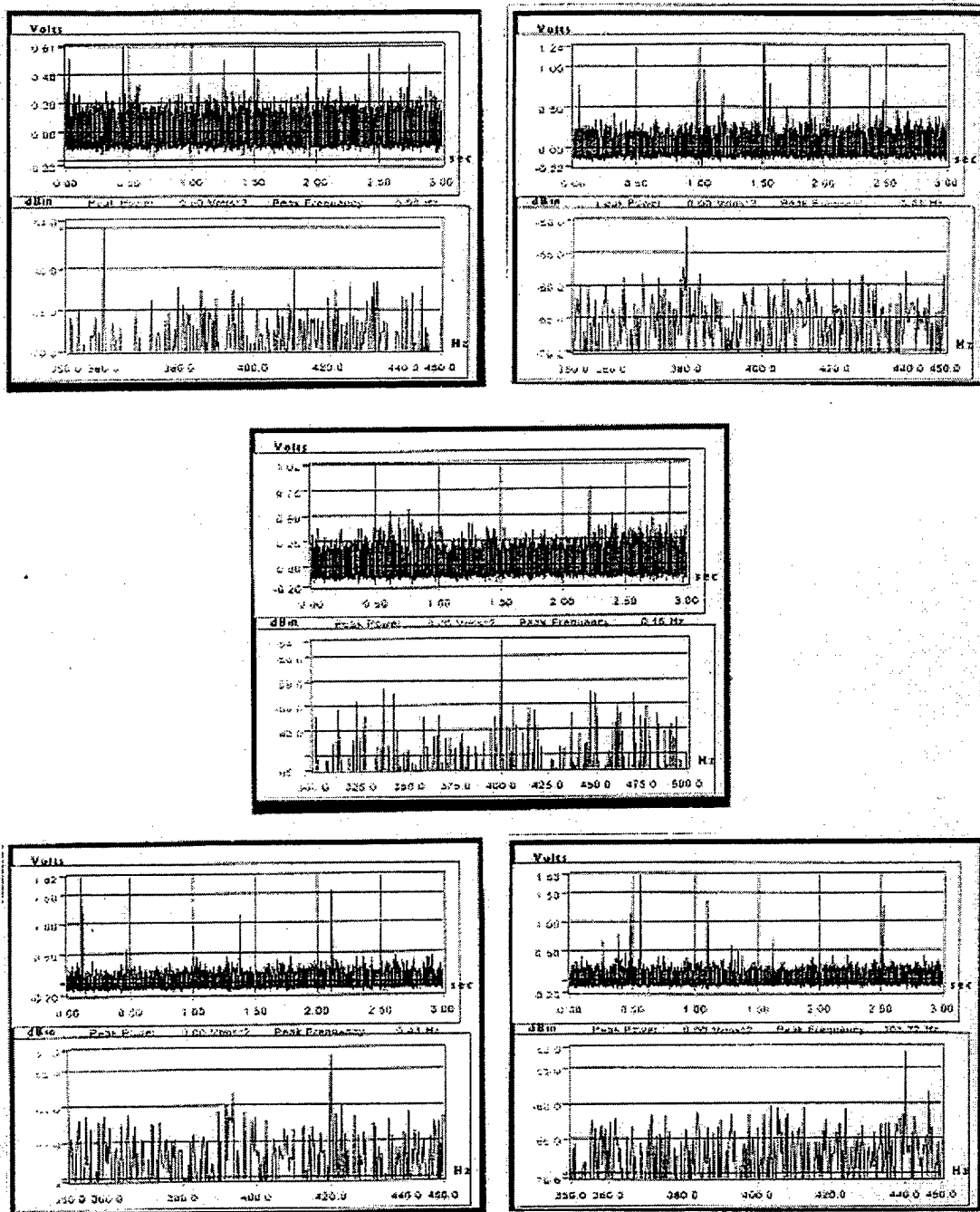


Fig. 17 Spectral target response at 360, 380, 400, 420 and 440 Hz.

## VI. CONCLUSIONS

Based on the limited measurements made with the modified system the following conclusions can be drawn:

The laser radar system is able to detect the vibrational frequencies in the target, given the output frequency spectrum on the computer, using a virtual instrument. The use of sample averaging signal processing was necessary to better discern the signal from the noise.

The optical alignment is a critical requisite to achieve a good signal response. Adjustment errors were always present, affecting the intensity of the beam at the detector. The optical system influences the range of the laser radar system. Much of the laser energy is lost in the beamsplitting process and wasted (producing hot spots on the fire bricks).

When the target vibration amplitude is increased, harmonics of the 400 Hz vibrating frequency appear in the spectrum. The estimation of the vibrational amplitude can be done depending of the appearance the respective harmonic.

The electronics circuitry improves the system CNR. The SNR is related to the target vibrational amplitude, and this relation can help in the process of target classification and identification. The power spectrum has a frequent and unexplained jump between -90 dB and -30 dB. The rise and fall of the power spectrum affect the SNR-to-vibrational amplitude target relation, making the analysis complex.

The stability of the target, a retroreflector bonded to a piezo electric actuator was a continuous problem, because it breaks frequently. The sensitivity of the detector was reduced motivated the addressing of errors in the optical alignment and hardware components, like the post-amplifier and the applied bias voltage. The mount to support the detector was modified to let it to have 3D movement.

The virtual instrument permits averaging of the signal, with low noise capabilities, and improving the carrier-to-noise ratio. To compare with the real instrument some of the data was printed using the traditional plotter and printer.

We fully expect that the vibrational signature can be used to identify some kinds of vehicles and aircraft. The ability to detect and identify targets is the principal area for further exploration and development of the laser radar system.



## **VII. RECOMENDATIONS**

The following changes to the system can result in improved performance:

- Increase the sensitivity using a liquid nitrogen cooled HgCdTe detector.
- Modify the optics to have better optical transmitting and receiving efficiency.
- Improve the detection range of the system by reducing the electronic bandwidth.
- Improve the analysis process of the signal using the software available.



## LIST OF REFERENCES

American National Safety Institute, ANZI Z136.1-1936, American National Standard For Safe Use of Lasers, The Laser Institute of America, New York, New York, 1993.

Chance, Thomas H., FM-CW Laser Radar at 10.6 Microns, Naval Postgraduate School Thesis, Monterey, California, 1974.

Day, James V., Construction of a Continuous Wave Frequency Modulated Laser Radar for use in Target Identification, Naval Postgraduate School Thesis, Monterey, California, 1997.

Fraunfelder, Maurice F. , A Heterodyne Detection FM-CW Laser Radar using a 10.6  $\mu\text{m}$  Source, Naval Postgraduate School Thesis, Monterey, California, 1974.

Harney, Robert C. , Laser Radar Systems: Theory, Technology, and Applications, Lecture Notes, Monterey, California, 1993.

Harney , Robert C. , The Rate Equation Theory of Lasers, Naval Postgraduate School Class Notes, Monterey, California, 1996.

Harney, Robert C. , Sensors and Devices, Naval Postgraduate School Class Notes, Monterey, California, 1996.

Jelalian, Albert V. , Laser Radar Systems, Artech House, Norwood, Massachusetts, 1992.

Johnson, Gary W. , LabVIEW Graphical Programming, McGraw-Hill Series, San Francisco, California, 1994.

Kamerman, Gary W., Applied Laser Radar Technology II, SPIE Proceedings Series, Vol. 2472, Orlando, Florida, 1995.

National Instruments, DAQ, PC-516 User Manual, Austin, Texas, 1996.

National Instruments, LabView, User Manual, Austin, Texas, 1996.

Schlessinger, Monroe, Infrared Technology Fundamentals, 2<sup>nd</sup> Edition, Marcel Dekker Inc., New York, New York, 1995.

Scruby, C. B., and Drain, L. E., Laser Ultrasonics: Techniques and Applications, Adam Hilger, Bristol, England, 1990.

Siegman, Antony E., Lasers, University Science Books, Sausalito, California, 1986.

Synrad Inc., Series 48 Lasers: Operation and Service Manual Version 2.1, Synrad Inc., Mukilteo, Washington, 1996.

Verdeyen, Joseph T., Laser Electronics, 3<sup>rd</sup> Edition, Prentice Hall, Englewood, Cliffs, New Jersey, 1995.

Wilson J., and Hawkes J. F. B., Optoelectronics, An Introduction, 2<sup>nd</sup> Edition, Prentice Hall, New York, New York, 1989.

## INITIAL DISTRIBUTION LIST

1. Defense Technical Information .....2  
8725 John J. Kingman Rd., Ste 0944  
Ft. Belvoir, VA 22060-6218
2. Dudley Knox Library .....2  
Naval Postgraduate School  
411 Dyer Rd.  
Monterey, CA 93943-5101
3. Professor Robert C. Harney (Code PH/Ha) .....3  
Naval Postgraduate School  
Monterey, CA 93943
4. Professor D. Scott Davis (Code PH/Ds) .....1  
Naval Postgraduate School  
Monterey, CA 93943
5. Chairman (Code PH).....1  
Department of Physics  
Naval Postgraduate School  
Monterey, CA 93943
6. Felix Montes .....3  
CCS-4287  
P.O. BOX 025323  
Miami, FL 33102-5323